International Journal of Mathematical Archive-8(6), 2017, 53-62
Available online through www.ijma.info ISSN 2229 – 5046

EFFECT OF HEAT SOURCES ON NON-DARCY CONVECTIVE HEAT AND MASS TRANSFER FLOW OF NANOFLUIDS IN CYLINDRICAL ANNULUS

C. SULOCHANA[1], G. N. RAMA KRISHNA*[2]

[1]Professor, Dept of Mathematics, Gulbarga University, Gulbarga, India.
[2]Scholar, Dept of Mathematics, Gulbarga University, Gulbarga, India.

Received On: 09-06-17; Revised & Accepted On: 27-06-17)

ABSTRACT

W*e analyze non-Darcy convective heat and mass transfer flow of nanofluids in a cylindrical annulus with heat sources and chemical reaction. By employing Galerkin finite element analysis with quadratic approximation functions the governing equations have been solved. The velocity, temperature and concentration have analyzed for G, D^{-1},Δ, α, γ, Sc and ϕ. Also the Skin friction and the rate of heat and mass transfer have been obtained for different parametric variations. It is found that the velocity and actual concentration reduces with increase in heat generating source and enhances with heat absorption source, while the temperature reduces with heat generating/absorption source.*

Keywords: *Heat Sources, non-Darcy, Nanofluid, Cylindrical annulus, Heat and Mass transfer.*

1. INTRODUCTION

Present days, researchers are more concentrating on enhancement of heat transfer. The low thermal conductivity of conventional heat transfer fluids, such as water, is considered a primary limitation in enhancing the heat transfer performance. Maxwell's review [19] demonstrated the possibility of increasing the thermal conductivity of fluid-solid particles. Subsequently, the particles with micrometer or considerably millimeter measurements were utilized. Those particles caused several problems such as abrasion, clogging and pressure losses. During the past decade the technology of producing particles in nanometer dimensions was improved and a new kind of solid-liquid mixture that is called nanofluid was established by Choi [5]. The dispersion of a small amount of solid nanoparticle in conventional fluids such as water or Ethylene glycol changes their thermal conductivity remarkably. In general, in most recent research areas, heat transfer enhancement in forced convection is desirable [3, 4 and 15], but there is still a debate on the effect of nano-particles on heat transfer enhancement in natural convection applications. Natural convection of Al_2O_3-water and CuO-water nanofluid inside a cylindrical enclosure heat from one side and cooled from the other side was studied by Putra *et al.*, [13]. They found that the natural convection heat transfer coefficient was lower than that of pure water. Wen and Ding [20] investigated the natural convection of TiO_2-water in a vessel composed of two discs. Their results showed that the natural convection decreases by increasing the volume fraction of nanoparticle. Jou and Tzeng [7] conducted a numerical study of natural convection heat transfer in rectangular enclosure filled with the stream function-vorticity formulation. They investigated the effects of Rayleigh number, the aspect ratio of the enclosure, and the volume fraction of the nanoparticle on the heat transfer inside the enclosures. Their results showed that the average heat transfer coefficient increased with increasing the volume fraction of the nanoparticle. Mokhtari Moghar*i et al.* [11] quested two phase mixed convection Al_2O_3-water nanofluid flow in an annulus. Thermal conductivity variation on natural convection flow of water-alumina nanofluid in annulus is investigated by Parvin *et al.* [14]. Soleimani *et al.* [16] studied natural convection heat transfer in a nanofluid filled semi-annulus enclosure. Abu-Nada *et al.* [1] studied natural convection heat transfer enhancement in horizontal concentric annuli using nanofluid. Abu-Nada [2] investigated the effect of variable viscosity and thermal conductivity of Al_2O_3-water nanofluid on heat transfer enhancement in natural convection. Das *et al* [6] have studied mixed convective magneto hydrodynamic flow in a vertical channel filled with nanofluids. Sreedevi *et al.* [19] has investigated mixed convective heat and mass transfer flow of nanofluids in concentric annulus with constant heat flux. NagaSasikala *et al.* [12] have investigated heat and mass transfer of a MHD flow of a nanofluid through a porous medium in an annular, circular region with outer cylinder maintained at constant heat flux. Sudarsana *et al.*, [18] have analyzed the Soret and Dufour effects on MHD convective flow of Al2O3-water and TiO2-water nanofluids past a stretching sheet in porous media with heat generation with heat generation/absorption. Recently Madhusudhana Reddy *et al.*, [8] have presented Numerical study of Convective Flow of CuO-water and Al_2O_3-water Nanofluids in cylindrical annulus.

Corresponding Author: G. N. Rama Krishna*[2]
[2]Scholar, Dept of Mathematics, Gulbarga University, Gulbarga, India.

In this paper we investigate non-Darcy convective heat and mass transfer flow of nanofluids in a cylindrical annulus with heat sources and chemical reaction. By employing Galerkin finite element analysis with quadratic appropriate functions the governing equations have been solved. The velocity temperature and concentration, Skin friction and the rate of heat and mass transfer have been obtained for different parametric variations.

2. FORMULATION OF THE PROBLEM:

We consider the free and forced convection flow in a vertical circular annulus through a porous medium whose walls are maintained at a constant heat flux and uniform concentration. The flow, temperature and concentration in the fluid are assumed to be fully developed. Both the fluid and porous region have constant physical properties and the flow is a mixed convection flow taking place under thermal and molecular buoyancies and uniform axial pressure gradient. The Boussinesq approximation is invoked so that the density variation is confined to the thermal and molecular buoyancy forces. The Brinkman-Forchheimer-Extended Darcy model which accounts for the inertia and boundary effects has been used for the momentum equation in the porous region. The momentum, energy and diffusion equations are coupled and non-linear. Also the flow is unidirectional along the axial direction of the cylindrical annulus.

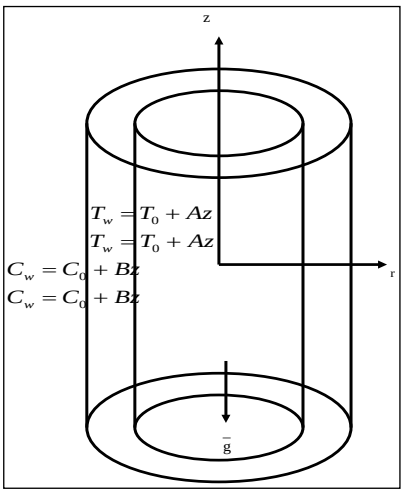

Fig.1*: C*onfiguration of the Problem

Making use of the above assumptions the governing equations are

$$-\frac{\partial p}{\partial z}+\frac{\mu_{nf}}{\rho_{nf}\delta}\left(\frac{\partial^2 u}{\partial r^2}+\frac{1}{r}\frac{\partial u}{\partial r}\right)-\left(\frac{\mu_{nf}}{k\rho_{nf}}\right)u-\frac{\delta F}{\rho_{nf}\sqrt{k}}u^2+\frac{(\rho\beta)_{nf}}{\rho_{nf}}(T-T_0)=0 \tag{1}$$

$$(\rho C_p)_{nf}\,u\frac{\partial T}{\partial z}=k_{nf}\left(\frac{\partial^2 T}{\partial r^2}+\frac{1}{r}\frac{\partial T}{\partial r}\right)-Q_H(T-T_0) \tag{2}$$

$$u\frac{\partial C}{\partial z}=D_B\left(\frac{\partial^2 C}{\partial r^2}+\frac{1}{r}\frac{\partial C}{\partial r}\right)-k_c^{'}C \tag{3}$$

where u is the axial velocity in the porous region, T, C are the temperature and concentration of the fluid, k is the permeability of porous medium, k_f is the thermal diffusivity, F is a function that depends on Reynolds number, the microstructure of the porous medium and D_B is the molecular diffusivity, β is the coefficient of the thermal expansion, Q_H is the heat source coefficient, Cp is the specific heat, ρ is density and g is gravity. $k_c^{'}$ is the coefficient of chemical reaction.

The relevant boundary conditions are

$u=0$, T= T_w, C= C_w at r = a & a+s (4)

Following Tao[19], and Das et al [6] we assume that the temperature and concentration of the both walls is $T_w = T_0 + Az$, $C_w = C_0 + Bz$ where A and B are the vertical temperature and concentration gradients which are positive for buoyancy –aided flow and negative for buoyancy –opposed flow, respectively, T_0 and C_0 are the upstream reference wall temperature and concentration , respectively. For the fully developed laminar flow in the presences of radial magnetic field, the velocity depend only on the radial coordinate and all the other physical variables

except temperature, concentration and pressure are functions of r and z, z being the vertical co-ordinate .The temperature and concentration inside the fluid can be written as

$$T = T^{\bullet}(r) + Az, \qquad C = C^{\bullet}(r) + Bz \tag{5}$$

The properties of nanofluid as follows,

$$\left.\begin{aligned} &\mu_{\mathrm{nf}} = \frac{\mu_{\mathrm{f}}}{(1-\varphi)^{2.5}}, \qquad \rho_{\mathrm{nf}} = (1-\varphi)\rho_{\mathrm{f}} + \varphi\rho_{\mathrm{s}}, \qquad \mathrm{k_{nf}} = \mathrm{k_f}\left[\frac{\mathrm{k_s} + 2\mathrm{k_f} - 2\phi(\mathrm{k_f} - \mathrm{k_s})}{\mathrm{k_s} + 2\mathrm{k_f} + \phi(\mathrm{k_f} - \mathrm{k_s})}\right] \\ &\alpha_{\mathrm{nf}} = \frac{\mathrm{k_{nf}}}{(\rho \mathrm{C_p})_{\mathrm{nf}}}, \quad (\rho \mathrm{C_p})_{\mathrm{nf}} = (1-\varphi)(\rho \mathrm{C_p})_{\mathrm{f}} + \varphi(\rho \mathrm{C_p})_{\mathrm{s}}, \ (\rho\beta)_{\mathrm{nf}} = (1-\varphi)(\rho\beta)_{\mathrm{f}} + \varphi(\rho\beta)_{\mathrm{s}} \end{aligned}\right\} \tag{6}$$

μ_{nf} is the dynamic viscosity of the nanofluid is, ρ_{nf} is the density of the nanofluid, $(\rho\beta)_{nf}$ is the thermal expansion of the nanofluid, $(\rho C_p)_{nf}$ is the heat capacitance of the nanofluid, α_{nf} is the coefficient of thermal diffusivity of the nanofluid. The subscripts nf, f and s represent the thermo physical properties of the nanofluid, base fluid and the nanosolid particles respectively and ϕ is the solid volume fraction of the nanoparticles. The thermo physical properties of the nanofluid are given in Table 1.

Table – 1

Physical Properties	Fluid phase	CuO (Copper)	Al_2O_3 (Alumina)	TiO_2 (Titanium dioxide)
C_p(j/kg K)	4179	385	765	686.2
ρ(kg m^3)	997.1	8933	3970	4250
k(W/m K)	0.613	400	40	8.9538
βx10^{-5} 1/k)	21	1.67	0.63	0.85

We now define the following non-dimensional variables

$$\left.\begin{aligned} &z^* = \frac{z}{a}, \ r^* = \frac{r}{a}, \ u^* = \left(\frac{a}{\nu}\right)u, \ p^* = \frac{pa\delta}{\rho\nu^2}, \\ &\theta^*(r^{\bullet}) = \frac{T^{\bullet} - T_0}{P_1 A a}, \ C^*(r^{\bullet}) = \frac{C^{\bullet} - C_0}{P_1 B a}, \ s^* = \frac{s}{a}, \ P_1 = \frac{dp}{dx} \end{aligned}\right\} \tag{7}$$

Introducing these non-dimensional variables, the governing equations in the non-dimensional form are (On removing the stars)

$$\left(\frac{\partial^2 u}{\partial r^2} + \frac{1}{r}\frac{\partial u}{\partial r}\right) = A_1 A_3 + \delta A_1 (D^{-1})u + \delta^2 A_1 \Delta u^2 - \delta A_1 A_4 G(\theta) \tag{8}$$

$$A_2\left(\frac{\partial^2 \theta}{\partial r^2} + \frac{1}{r}\frac{\partial \theta}{\partial r}\right) = A_5 P_r u - \alpha\theta \tag{9}$$

$$\left(\frac{\partial^2 C}{\partial r^2} + \frac{1}{r}\frac{\partial C}{\partial r}\right) - \gamma C = Sc\, u \tag{10}$$

Where

$\Delta = FD^{-1/2}$ (Inertia parameter or Forchheimer number), $G = \dfrac{g\beta(T_e - T_i)a^3}{\nu^2}$ (Grashof number)

$D^{-1} = \dfrac{a^2}{k}$ (Inverse Darcy parameter), $\alpha = \dfrac{Qa^2}{k_f C_p}$ (Heat Source parameter),

$P_r = \dfrac{\mu C_p}{k_f}$ (Prandtl number) $Sc = \dfrac{\nu}{D_B}$ (Schmidt number),

$\gamma = \dfrac{k_c^1 a^2}{D_B}$ (Chemical Reaction parameter) $A_1 = (1-\varphi)^{2.5}$,

$$A_2 = \frac{k_{nf}}{k_f}, \qquad A_3 = (1-\varphi) + \varphi\left(\frac{\rho_s}{\rho_f}\right),$$

$$A_4 = (1-\varphi) + \varphi\left(\frac{(\rho\beta)_s}{(\rho\beta)_f}\right), \qquad A_5 = (1-\varphi) + \varphi\left(\frac{(\rho C_p)_s}{(\rho C_p)_f}\right)$$

The corresponding non-dimensional conditions are

$u = 0 \quad \theta = 0$ C=0 at r=1 and 1+s (11)

3. METHOD OF SOLUTION

The finite element analysis with quadratic polynomial approximation functions is carried out along the radial distance across the circular duct. The behavior of the velocity, temperature and concentration profiles has been discussed computationally for different variations in governing parameters. The Galerkin method has been adopted in the variational formulation in each element to obtain the global coupled matrices for the velocity, temperature and concentration in course of the finite element analysis.

Choose an arbitrary element e_k and let u^k, θ^k and C^k be the values of u, θ and C in the element e_k. We define the error residuals as

$$E_p^k = \frac{d}{dr}\left(r\frac{du^k}{dr}\right) + \delta A_1 A_4 G(\theta^k) - \delta A_1 (D^{-1}) r u^k - \delta^2 \Delta r (u^k)^2 - A_1 A_3 \tag{12}$$

$$E^k{}_\theta = A_2 \frac{d}{dr}\left(r\frac{d\theta^k}{dr}\right) - A_5 P_R r u^k - \alpha r\theta \tag{13}$$

$$E^k{}_c = \frac{d}{dr}\left(r\frac{dC^k}{dr}\right) - rScu^k - \gamma C^k \tag{14}$$

Where u^k, θ^k & C^k are values of u, θ& C in the arbitrary element e_k. These are expressed as linear combinations in terms of respective local nodal values.

$$u^k = u_1^k\psi_1^k + u_2^k\psi_1^k + u_3^k\psi_3^k, \qquad \theta^k = \theta_1^k\psi_1^k + \theta_2^k\psi_2^k + \theta_3^k\psi_3^k \qquad C^k = C_1^k\psi_1^k + C_2^k\psi_2^k + C_3^k\psi_3^k \tag{15}$$

Where ψ_1^k, ψ_2^k …..etc... are Lagrange's quadratic polynomials.

Galerkin's method is used to convert the partial differential Eqs. (12) – (14) into matrix form of equations which results into 3x3 local stiffness matrices. All these local matrices are assembled in a global matrix by substituting the global nodal values of order I and using inter element continuity and equilibrium conditions.

The shear stress (τ), Nusselt number (rate of heat transfer), Sherwood number (rate of mass transfer) are evaluated by using the following formulas

$$\tau = \left(\frac{du}{dr}\right)_{r=1,1+s}, \qquad Nu = -\left(\frac{d\theta}{dr}\right)_{r=1,1+s}, \qquad Sh = -\left(\frac{dC}{dr}\right)_{r=1,1+s}$$

Comparison: In the absence of absence of Heat sources (α=0) the results are in good agreement with Madhusudhana Reddy *et al* [8].

Table-2: Nusselt Number (Nu) at r = 1 & 2

	Reddy et al [8]		Present Results		Reddy et al[8]		Present Results	
ϕ	Cuo-Water		Cuo-Water		Al_2O_3-Water		Al_2O_3-Water	
	Nu (1)	**Nu (2)**	**Nu (1)**	**Nu (2)**	**Nu (1)**	**Nu (2)**	**Nu (1)**	**Nu (2)**
0.05	0.233577	-0.20696	0.233607	-0.20689	0.241851	-0.199721	0.241901	-0.199801
0.1	0.163482	-0.12083	0.163528	-0.12103	0.185224	-0.092153	0.185314	-0.092193
0.3	0.136183	-0.10503	0.136203	-0.10516	0.159538	-0.072082	0.159608	-0.072102
0.5	0.103455	-0.09287	0.103525	-0.09296	0.104786	-0.046868	0.104826	-0.046928

4. IMPORTANT RESULTS AND CONCLUSIONS IN THIS ANALYSIS

The equations governing the flow, heat and mass transfer have been solved by employing Galerkin finite element analysis with quadratic approximation polynomials. We have chosen here Pr= 6.2 while α, Sc, γ, ϕ and Δ are varied over a range, which are listed in the Figure legends.

Effects of parameters on velocity profiles:

Fig. 2 depicts the behavior of the velocity with heat source parameter α. It is found that magnitude of axial velocity decreases with increase in the strength of the heat generating source. This is due to the fact that when heat is absorbed, the buoyancy forces increases which reduces the flow rate and there by gives rise to depreciation in the velocity profile. An increase in the heat absorbing heat source increases the axial velocity in the entire flow region in both types of nanofluid. We also find that the values of velocity in CuO-water nanofluid are relatively lesser than those of Al_2O_3-water nanofluid. Also u exhibits a reversal flow in the central core of the flow region ($1 \leq r \leq 1.7$). The region of reversal flow reduces with increase in $\propto>0$ and enhances with $\propto<0$. Fig.3 displays the effect of nanoparticle volume fraction ϕ on the nanofluid velocity. It is found that as the nanoparticle volume fraction decreases the magnitude of nanofluid velocity in both types of nanofluids. These figures illustrate this agreement with the physical behavior. When the volume of the nanoparticle reduces the thermal conductivity and hence reduces the momentum boundary layer thickness.

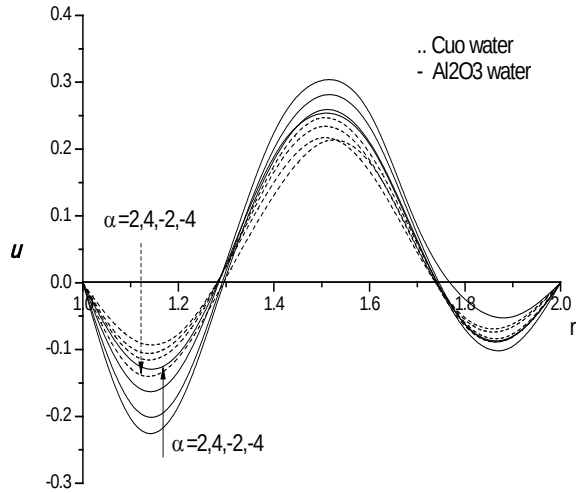

Fig. 2: Variation of u with α

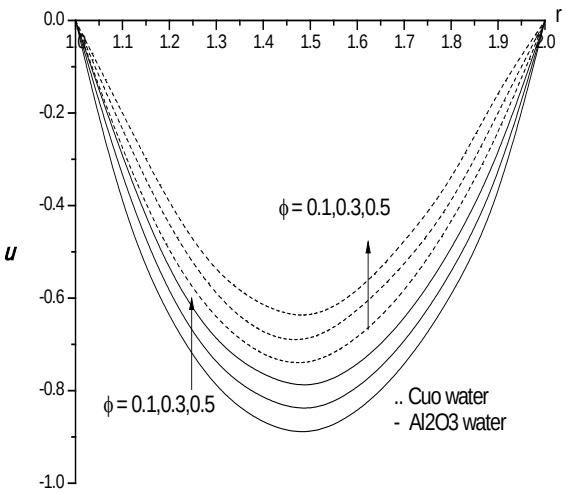

Fig. 3: Variation of u with ϕ

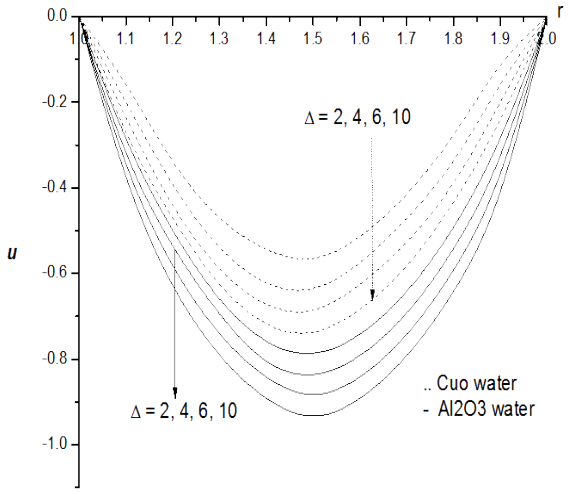

Fig. 4: Variation of u with Δ

The variation of velocity with Forchheimer number Δ is exhibited in Fig.4. It is found that the magnitude of velocity shows an enhancement with increasing the values of Forchheimer number Δ in the flow region. This is due to the fact that the thickness of the boundary layer increases with values of Δ in both types of nanofluid.

Effects of parameters on temperature profiles:

Fig.5 depicts the behavior of the temperature with heat source parameter α. It is found that temperature exhibits a decreasing tendency with increase in the strength of the heat generating/absorbing source. This is due to the fact that the presences of the heat source generate/absorbing energy in the thermal boundary layer and as a consequence the temperature rises in the annular region. Fig. 6 shows that the variation of temperature with ϕ. It can be seen from the profiles that an increase in the nanoparticle volume fraction reduces the temperature in the boundary layer. This is due to the fact that the thickness of the thermal boundary layer decreases with increase in ϕ.

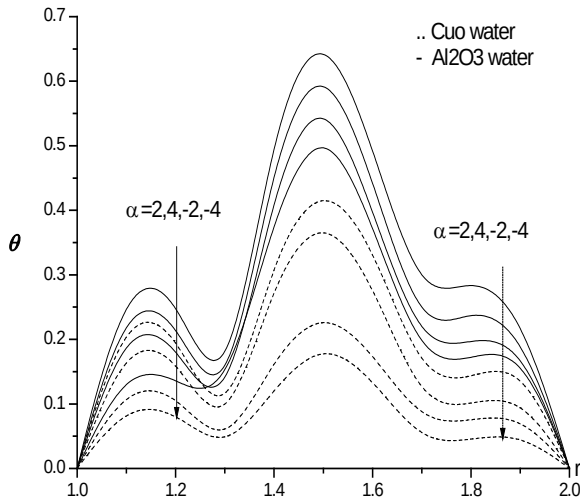

Fig. 5: Variation of θ with α

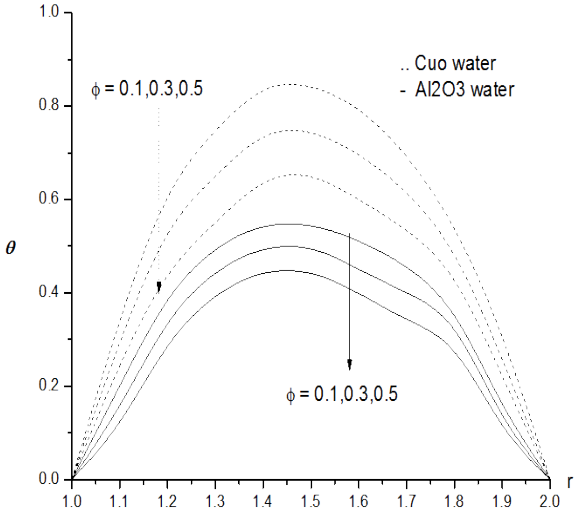

Fig. 6 : Variation of θ with ϕ

.

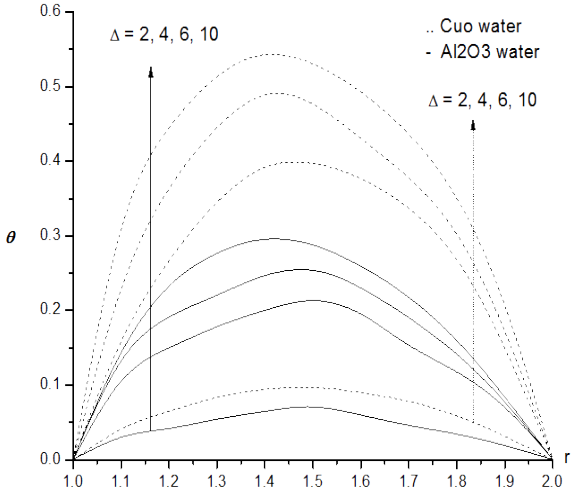

Fig. 7: Variation of θ with Δ

Also Fig. 7 shows the variation of temperature withΔ. It is found that an increase in Δ enhances the temperature in the thermal boundary layer, thus lesser the thermal diffusivity larger the temperature in the flow region.

Effects of parameters on concentration profiles:

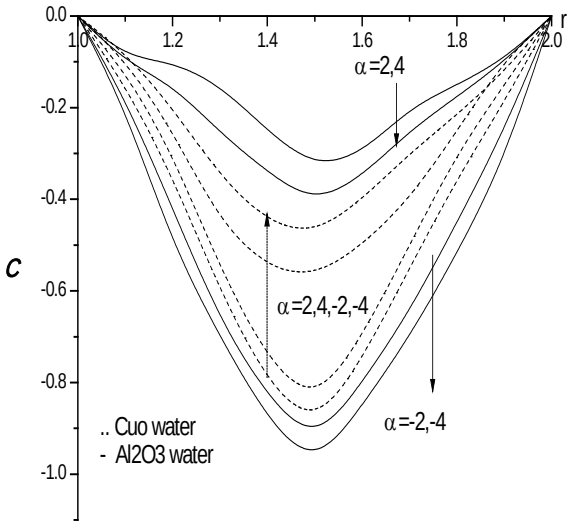

Fig. 8 : Variation of C with α

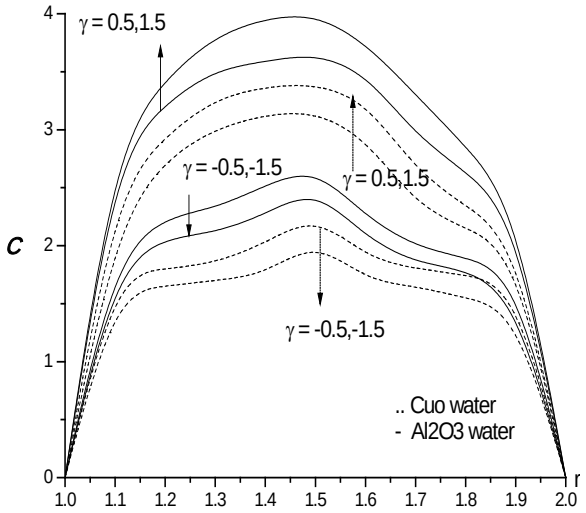

Fig. 9 : Variation of C with γ

Figure 8 represents the concentration (C) with heat source parameter α. In this case the actual concentration is negative. This implies that the actual concentration C is less than the equilibrium concentration C_0. The actual concentration reduces with increase in strength of the heat generating source ($\propto$>0) and increases with that of heat absorbing source. Fig. 9 represents the concentration (C) with chemical reaction parameter (γ). It can be seen from the concentration profiles that the actual concentration enhances in degenerating chemical reaction case and in the generating chemical reaction case we notice depreciation in the actual concentration in both types of nanofluid.

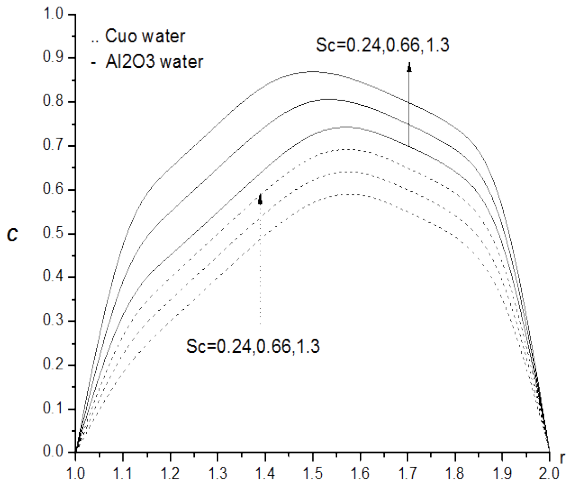

Fig. 10 : Variation of C with Sc

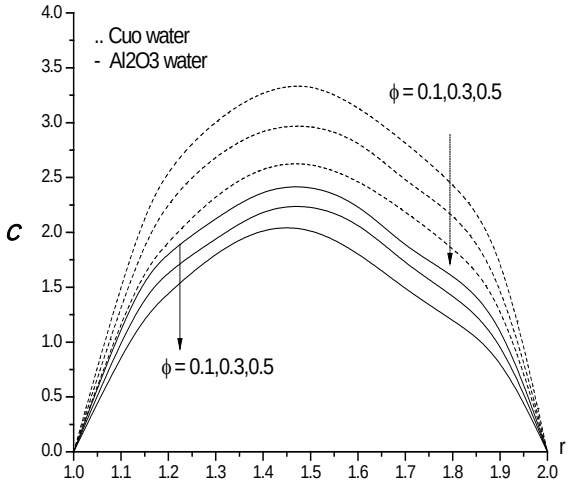

Fig. 11 : Variation of C with ϕ

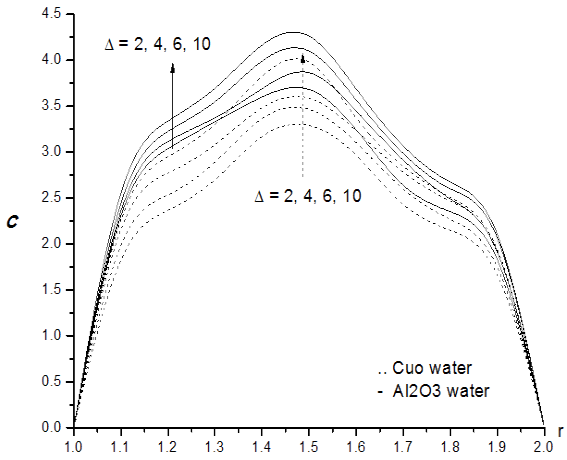

Fig. 12 : Variation of C with Δ

Fig.10 represents the variation of C with Sc. It is found that increase in Sc enhances the actual concentration in the fluid region in both types of nanofluid. Thus, lesser the molecular diffusivity larger the actual concentration in the flow region. Fig. 11 shows the variation of concentration with nanoparticle volume fraction ϕ.We notice a reduction in the actual concentration with increasing ϕ. This may be attributed to the fact that an enhancement in ϕ results in decreasing the thickness of the solutal boundary layer. The concentration in CuO-water nanofluid is greater than those values in Al_20_3-water nanofluid. Fig. 12 depicts the concentration withΔ. It can be seen from the profiles that the actual concentration enhances with increase inΔ. This shows that higher the Forchheimer number larger the thickness of the solutal boundary layer.

Effects of parameters on Skin friction:
The skin friction on inner and outer cylinders is exhibited in table 3 for different parametric variations.

Table -3: Skin Friction (τ) and Nusselt Number (Nu) at the boundaries r = 1 and 2

	Cuo-water		**Al_2O_3-water**	
	τ(1)	**τ(2)**	**Nu (1)**	**Nu (2)**
$\propto$ 2	-0.344709	0.295543	-0.375427	0.309548
4	-0.353567	0.299686	-0.383641	0.326910
-2	-0.363166	0.245654	-0.393429	0.256453
-4	-0.384333	0.252341	-0.399738	0.296603
ϕ 0.05	-0.344709	0.295543	-0.375427	0.309548
0.1	-0.322286	0.234133	-0.356835	0.243367
0.3	-0.298190	0.199080	-0305607	0.155813
0.5	-0.166095	0.166046	-0.204787	0.125445
Δ 2	-0.344709	0.295543	-0.375427	0.309548
4	-0.835576	0.757665	-0.904463	0.866134
6	-1.793485	1.213450	-1.855349	1.234368
10	-2.329867	2.148234	-2.454894	2.357145

Higher the strength of heat generating/absorbing source larger $|\tau|$ at both the cylinders. An increase in the nanoparticle volume fraction ϕ reduces $|\tau|$ at the cylinders in both types of nanofluid. The stress enhances at r= 1 and 2 with an increase in Forchheimer number (Δ) for both types of nanofluid. In all the above variations we noticed that the values of stress in Cuo-water nanofluid are relatively smaller than those in Al_2O_3-water nanofluid.

Effects of parameters on Nusselt Number:
The rate of heat transfer (Nusselt Number (Nu)) at the inner and outer cylinders is shown in table 4 for different parametric variations

Table -4

	Cuo-water		**Al_2O_3 -water**	
	Nu (1)	**Nu (2)**	**Nu (1)**	**Nu (2)**
α 2	0.235577	-0.216962	0.217655	-0.209721
4	0.257066	-0.225774	0.225154	-0.222175
-2	0.226042	-0.188545	-0.213534	-0.176137
-4	0.205036	-0.164543	-0.179857	-0.156076
ϕ 0.05	0.235577	-0.216961	0.217655	-0.209721
0.1	0.193482	-0.120833	0.175224	-0.112153
0.3	0.146183	-0.105038	0.129538	-0.099082
0.5	0.113455	-0.092879	0.104786	-0.077868
Δ 2	0.235577	-0. 216962	0.217655	-0.209721
4	0.864484	-1.291456	0.669542	-1.034882
6	1.451445	-4.642634	1.228413	-3.001753
10	2.661746	-5.630959	2.358894	-4.055524

An increase in the strength of the heat generating source enhances |Nu| while it reduces with that of heat absorbing source at r = 1 & 2. An increase in nanoparticle volume fraction ϕ reduces the rate of heat transfer at r = 1 & 2 in both types of nanofluid. The variation of Nu with Forchheimer number Δ shows that the rate of heat transfer enhances with increase in Δ. Thus inclusion of inertia of boundary effects leads an enhancement in the rate of heat transfer. In all the above variations we noticed that the values of Nu in Cuo-water nanofluid are relatively greater than those in Al_2O_3-water nanofluid.

Effects of parameters on Sherwood Number:

The table 5 represents the variation of mass transfer Sh at r=1&2 with different values of α, Sc, γ, ϕ and Δ.

Table – 5: Sherwood Number (Sh) at the boundaries r = 1 and 2

		Cuo-water		**Al_2O_3-water**	
		Sh (1)	**Sh (2)**	**Sh (1)**	**Sh (2)**
α	2	0.255986	-0.198652	0.220067	-0.166353
	4	0.260395	-0.258563	0.254633	-0.194069
	-2	-0.787312	0.187312	-0.188339	0.149601
	-4	-0.785074	0.177789	-0.150703	0.1282227
Sc	0.24	0.104446	-0.075289	0.040627	-0.029419
	0.66	0.171228	-0.099546	0.112133	-0.081194
	1.3	0.255986	-0.198652	0.220067	-0.166353
γ	0.5	0.255986	-0.198652	0.220067	-0.166353
	1.5	0.265453	-0.230036	0.246593	-0.178267
	-0.5	0.133478	-0.242815	0.118714	-0.144114
	-1.5	0.090521	-0.221693	0.081158	-0.131572
ϕ	0.05	0.255986	-0.198652	0.220067	-0.166353
	0.1	0.186332	-0.107717	0.156509	-0.077296
	0.3	0.164165	-0.099089	0.104996	-0.033426
	0.5	0.095028	-0.066309	0.081252	-0.025530
Δ	2	0.255986	-0.198652	0.220067	-0.166353
	4	0.728326	-0.482636	0.534066	-0.386715
	6	1.333964	-0.921456	1.160693	-0.840484
	10	1.897371	-1.719998	1.690751	-1.586456

The table 5 represents the variation of mass transfer (Sh) at r=1&2 with different values of α, Sc, γ, ϕ and Δ. The rate of mass transfer increases with increase in heat generating source and reduces with that of heat absorbing source at both the cylinders in both types of nanofluid. With respect to Schmidt number (Sc) we notice an enhancement in |Sh| at the cylinders in both fluids. The variation of Sh with chemical reaction parameter (γ) shows that the rate of mass transfer enhances in the degenerating chemical reaction case and reduces in the generating chemical reaction case at the cylinders in both types of nanofluid. An increase in the nanoparticle volume fraction ϕ reduces |Sh| at r= 1 & 2 in both fluids. The rate of mass transfer enhances with increase in Forchheimer number (Δ). This indicates that inclusion of inertia and boundary effects leads to an enhancement in |Sh| at both cylinders. . It is found that in all the variations the values of Sherwood number in Cuo-water nanofluid are remarkably greater than those values in Al_2O_3-water nanofluid.

CONCLUSIONS

- An increase in α>0 reduces the Velocity, temperature and actual concentration. The velocity and actual concentration enhances and temperature reduces with α<0. The skin friction enhances with |α| while the rate of heat and mass transfer enhances with α>0 and reduces with α<0.
- An increase in nanoparticle volume fraction ϕ reduces the velocity, temperature and actual concentration. The skin friction, the rate of heat and mass transfer reduces ϕ at both the cylinders.
- Lesser the molecular diffusivity larger the actual concentration and rate of mass transfer.
- The actual concentration enhances and Sherwood number increases at r = 1 & 2 in the degenerating chemical reaction case, while in the generating chemical reaction case a reversed effect is observed in C and Sh.
- An increase in Forchheimer number (Δ) leads to an enhancement in |u|, θ and C. τ, Nu and Sh increases with Δ at r= 1 & 2 in both nanofluids.

5. REFERENCES

1. Abu-Nada, E., Masoud, Z., Hijazi, A: Natural convection heat transfer enhancement in horizontal concentric annuli using nanofluids, Int Commun Heat Mass Transf, V.35, 657-665(2008).
2. Abu-Nada, E: Effect of variable viscosity and thermal conductivity of Al_2O_3-water nanofluid on heat transfer enhancement in natural convection, Int J heat Fluid Flow, V.30, 679-690(2009).
3. Behzadmehr, A., Saffar-Avval, M., Galanis, N: Prediction of turbulent forced convection of a nanofluid in a tube with uniform heat flux using a two phase approach, Int J Heat Fluid Flow, V.28, 211-219(2007).
4. Bianco V., Chiacchio. F., Manca, O., Nardini, S: Numerical investigation of nanofluids forced convection in circular tubes, J. Appl Therm Eng, V.29, 3632-3642(2009).

5. Choi, S.U.S: Enhancing thermal conductivity of fluid with nanoparticles, developments and applications of non-Newtonian flow, ASME FED 231, 99-105(1995).
6. Das, S., Jana, R.N., and Makinde, O.D : Mixed convective magneto hydrodynamic flow in a vertical channel filled with nanofluids, Engineering science and technology an International Journal, V.18,pp.244-255(2015).
7. Jou, R.Y., Tzeng, S.C: Numerical research of nature convective heat transfer enhancement filled with nanofluids in rectangular enclosures, Int Commun Heat Mass Transf, V.33, 727-736(2006).
8. Madhusudhana Reddy, Y., Rama Krishna, G.N. and Prasada Rao, D.R.V: Numerical study of Convective Flow of CuO-water and Al_2O_3-water nanofluids in cylindrical annulus, Int. Journal of Research & Development in Tech., Vol. 7, Issue 3, pp. 142-148 (2017).
9. Maxwell, J.C: Electricity and magnetism, Clarendon Press, Oxford, UK (1873).
10. Putra, N., Roetzel W, Das, S.K: Natural convection of nanofluids, Heat and Mass Transfer, V.39 (8-9), 775-784(2003).
11. Mokhtari Moghari, R., Akbarinia, A., Shariat, M., Talebi, F., Laur, R: Two phase mixed convection Al_2O_3-water nanofluid flow in an annulus, Int J Multiph Flow, V.37(6), 585-595(2011).
12. Nagasasikala, M and Phrabhakar Rao G: Heat and mass transfer of a MHD flow of a nanofluid through a porous medium in an annular, circular region with outer cylinder maintained at constant heat flux, Presented in NCIT Conference, SSBN Degree College, Ananatapuramu(2016).
13. Putra, N., Roetzel W, Das, S.K: Natural convection of nanofluids, Heat and Mass Transfer, V.39 (8-9), 775-784(2003).
14. Parvin, S., Nasrin, R., Alim, M.A., Hossain, N.F., Chamka, A.J: Thermal conductivity variation on natural convection flow of water-alumina nanofluid in an annulus, Int J Heat Mass Transf, V.55 (19-20), 5268-5274(2012).
15. Santra, A.K., Sen, S., Chakraborty., N: Study of heat transfer due to laminar flow of copper-water nanofluid through two iso-thermally heated parallel plates, Int J Therm Sci., V.48, 391-400(2009).
16. Soleimani, S.I., Sheikholeslami, M., Ganji, D.D., Gorji-Bandpay, M: Natural convection heat transfer in a nanofluid filled semi annulus enclosure, Int Commun Heat Mass Transf, V.39 (4), 565-574(2012).
17. Sree devi , G., Raghavendra Rao, R., Chamka, A.J and Prasada Rao, D.R.V: Mixed convective heat and mass transfer flow of nanofluids in concentric annulus with constant heat flux, Procedia Engineering, 127, 1048-1055(2015).
18. Sudarsana Reddy, P., Chamka, A.J: Soret and Dufour effects on MHD convective flow of Al2O3-water and TiO2- water nanofluids past a stretching sheet in porous media with heat generation/absorption, J. Advanced Powder Technology, V. 27, 1207-1218(2016).
19. Tao, L.N: On combined and forced convection in channels, ASME J. Heat Transfer, V.82, pp.233-238 (1960).
20. Wen, D and Ding, Y: Formulation of nanofluids for natural convective heat transfer applications, Int J Heat Fluid Flow, V. 26(6), 855-864(2005).

Source of support: Nil, Conflict of interest: None Declared.